

PERSPECTIVE • OPEN ACCESS

Prospects on ultrasound measurement techniques with optical fibers

To cite this article: Xiaoyi Bao 2023 *Meas. Sci. Technol.* **34** 051001

View the [article online](#) for updates and enhancements.

You may also like

- [Transcranial ultrasound imaging with speed of sound-based phase correction: a numerical study](#)
Tianren Wang and Yun Jing
- [Piezoelectric bimorph-driven ultrasound scanner for high frequency ultrasound imaging](#)
Liyuan He, Zhiyi Wen, Boquan Wang et al.
- [Mechanism modeling for phase fraction measurement with ultrasound attenuation in oil–water two-phase flow](#)
Qian Su, Chao Tan and Feng Dong

Perspective

Prospects on ultrasound measurement techniques with optical fibers

Xiaoyi Bao 

Fiber Optics Group, Physics Department, University of Ottawa, Ottawa, ON K1N 6N5, Canada

E-mail: xbao@uottawa.ca

Received 20 September 2022, revised 29 December 2022

Accepted for publication 24 January 2023

Published 1 February 2023



CrossMark

Abstract

Ultrasound sensors have been widely used in medical imaging, as well as structural health monitoring (SHM) and non-destructive testing (NDT) in civil and mechanical structures. Covering entire structures and imaging large areas requires multiplexing of many ultrasound sensors with single readout instrument, which can be difficult for traditional piezoelectric transducers. Optical fiber-based sensors offer numerous advantages such as being lightweight, small, the ability to be embedded, immunity to electro-magnetic interference, and the ability to be multiplexed and distributed ultrasound sensors. Fiber ultrasound sensors are regarded as an ideal sensing solution for SHM and NDT, and even most recently for medical imaging due to its broadband ultrasound response and distributed capability. Micro and nanofibers are made smaller than telecom fibers using a wider selection of sensing materials with higher bending capability, which makes them ideal for high frequency (hundreds of MHz) ultrasound detection of micrometer cracks and imaging biological tissues. New optical materials and fabrication techniques are shaping the future with exceptionally small ultrasound sensors and actuators, extending the range of applications in SHM, NDT and medical imaging with higher accuracy and better precision over larger areas.

Keywords: optical fiber ultrasound sensors, structural health monitoring and non-destructive testing by ultrasound probe, ultrasound sensing for medical imaging, micro and nano fiber for ultrasound transmitter, laser ultrasound generation, multiplexing and distributed ultrasound sensors

(Some figures may appear in colour only in the online journal)

1. From optical sonometer to ultrasound sensors and their applications

2023 is the centennial year for ‘The optical sonometer’ paper published in the first issue of the Journal of Scientific Instruments [1]. The principle is simple: sound waves

collected by a horn fall on a silvered celluloid diaphragm of 18 mm in diameter and less than a wavelength of light in thickness as illustrated in figure 1. The core of the optical sonometer is a transducer: the reflecting diaphragm, which converts variations in sound-pressure into mechanical movement is recorded through optical means. The mechanical movements represent ultrasound and acoustic emission waves propagating through rigid structures and being subject to fast forced variation.

A sonometer is a diagnostic instrument that records the tension, frequency, or density of vibrations. During the past century, acoustic and ultrasound detection have been established



Original content from this work may be used under the terms of the [Creative Commons Attribution 4.0 licence](https://creativecommons.org/licenses/by/4.0/). Any further distribution of this work must maintain attribution to the author(s) and the title of the work, journal citation and DOI.



Figure 1. The general appearance of an optical sonometer. Reproduced from [1]. © IOP Publishing Ltd All rights reserved.

as valuable tools for imaging structures from a molecular scale for medical diagnosing, to monitoring the health conditions of civil and mechanical infrastructures. In medical ultrasound, an ultrasound pulse is transmitted into the body and is reflected due to the interfaces between tissues with different acoustic impedances to produce an image of different contrast, which carries the physiological and pathological information inside tissues. Ultrasound is an emerging measurement technique in biomedical imaging, photoacoustic sensing, and non-destructive industrial monitoring because of its non-invasive, non-destructive, and real-time monitoring capabilities [2].

Normal ultrasound imaging system can only reach 1 mm level resolution. However, high-frequency ultrasound (>20 MHz), which are only available in research centers allows for resolution of <100 μm for biomedical imaging, such as endoscopy, ophthalmology, intra-vascular image and dermatology [3].

Magnetic resonance imaging (MRI) systems have resolution of 1–2 mm [4]. In these systems, the intensity of detected MRI signal from an interrogated object strongly depends on the strength of the magnetic field of the imager's magnet. Imaging at lower resolutions thus would reduce the cost, size and weight of the MRI scanner and shorten image acquisition times. MR with ultrahigh magnetic field can reach resolution better than 100 μm .

In addition to being expensive, MRI systems have limited temporal resolution, which prevents fast imaging and rapid diagnosis. X-ray computed tomography is a relatively affordable modality with high resolution (400 μm); however, the ionizing radiation makes it unsafe for medical monitoring.

Multiple methods have been developed in several stages, both in generation and detection for specific frequency ranges and strengths (also called displacement) of mechanical movement, most relying on electrical systems. An important transition was accomplished by extending the use of electrical waveguides [lead-zirconate-titanate (PZT)] to optical waveguides, such as telecom fibers, micro and nanofibers. Highly sensitive ultrasound sensors with a broadband frequency response, ranging from kilohertz to a few hundreds MHz have been developed with the advancement of the detection

sensitivity and higher spatial resolution. These have been applied in several fields, such as biomedical imaging [3, 5] where optical ultrasound sensors can be used as probes to detect optical absorption by sound/acoustic wave, which offers unique capabilities in studying biological tissue [4]. The sensitivity and bandwidth of detecting laser-induced ultrasonic signals are crucial for attaining high quality and high-resolution medical images [6].

Structural health monitoring (SHM) [7] is the continuous monitoring of a structure's integrity under stress/strain, which is often performed with non-destructive testing (NDT) tools [8]. SHM can assess the condition of a structure through the monitoring of its in-service performance. SHM can detect deterioration in a structure to avoid catastrophic failures by predicting when a structure may collapse and thus be unsuitable for further use until maintenance work is performed. This process can minimize maintenance costs and the downtimes of critical structures, and hence provides a very high return on investment [7]. Small levels of damage can be detected by ultrasonic sensors based on acoustic guided waves (GW) [9]. Ultrasound and acoustic emissions have contributed to public safety and improved the quality of people's lives with their development through technological advancement.

Mechanical waves can be described by the phase and amplitude as a function of time. The low mechanical amplitude of the vibrations makes the recording process to be difficult, as the oscillation frequency occurs between 20 kHz to many MHz. If we increase the mechanical frequency of oscillation, the structure starts to behave like a low pass filter for which the higher frequencies are attenuated at a significant rate. Depending on the transducer medium, the amplitude can reach nano-strain ($n\epsilon$) levels for frequency higher than 1 MHz. This amplitude level is usually restricted to the surface of the structure and is only detectable with high-sensitivity sensing systems. The key challenge to the measurement of GWs with any sensor is the need of a high signal-to-noise ratio (SNR), so that the waveform can be well resolved within the acoustic wavelength.

An acoustic wave (mechanical wave) is an oscillation of pressure that travels through a solid, liquid, or gas in a wave

pattern [10]. It transmits sound by vibrating organs in the ear that produce the sensation of hearing. Also called sound waves, they are defined by three characteristics: wavelength, frequency, and amplitude. Wavelength is the distance from the top of one wave's crest to the next. Frequency is the number of waves that pass a point each second. Sound waves with higher frequencies have higher pitches than those with lower frequencies. Ultrasonic waves are acoustic waves with frequencies higher than human hearing range, so the terms 'ultrasonic' and 'acoustic' are often used interchangeably in the literature. Amplitude is the measure of energy in a wave and affects its volume. Greater amplitude means stronger pressure oscillation, which lead to louder sounds.

A device must be as small as an acoustic wavelength depending on the frequency of the ultrasound wave (20 kHz to tens of MHz). The associated acoustic wavelength varies from mm (larger structures) [7] to micrometres or sub- μm for high-resolution biomedical imaging, scientific research for drug development, medical diagnosis and NDT of microelectronic components [11]. Such a resolution requires a high-frequency ultrasound probe over broadband response.

Since Kao and Hockham [12] suggested optical fibers for communication systems, modulating the light within fibers by changing the refractive index has been investigated [13], which formed the foundation for optical fiber sensors (OFSs). OFSs offer significant advantages over other sensing methodologies, such as higher sensitivity, smaller size (diameter is hair thin), lightweight, immunity to electromagnetic interference and multiplexing with large numbers of sensing probes. Distributed ultrasound sensors have been demonstrated based on Rayleigh scattering using pencil break induced impact wave for the frequency range of kHz–10 MHz [14]. The high frequency components are detected by optical interferometers, while the location of the ultrasound signal is determined by optical time domain reflectometry (OTDR) technique using telecom fiber [15]. The simple structure of modifying single pulse OTDR with combined multiple long and short pulse [16] can also achieve distributed ultrasound sensor with spatial resolution of meters in frequency of sub-MHz range. They are ideal for NDT and SHM using telecom fibers.

Since the fiber is an optical waveguide device for light propagation, it is also an ideal ultrasound waveguide for high frequency ultrasound wave propagation with low loss over tens of meters [17], making them ideal for sensing acoustic/ultrasound signals for various applications. If an ultrasonic wave is guided by an optical fiber, which is then detected by a piezoelectric sensor, the leakage of a pipeline can be evaluated depending on additional ultrasonic attenuation [18]. Note this only works for short lengths ($<100\text{ m}$). One major advantage of OFSs is that light properties are changed in the presence of acoustic waves, and light itself propagates through the fiber carrying the acoustic information with extremely small attenuation. While acoustic waves can propagate in fibers and be detected by piezoelectric sensors close to the sensing point ($<100\text{ m}$), fiber-based ultrasound sensors with telecom fiber offers remote sensing over kilometers [15, 16]. In addition, multiplexing point fiber sensors can achieve simultaneous ultrasound measurement in multiple locations [19, 20].

2. Ultrasound detection by lead-zirconate-titanate (PZT) and optical waveguide sensors

The change of refractive index in a material due to an applied strain is called the strain-optic effect [21]. The acoustic signal is a pressure wave in the material in the form of an elastic wave, known as a stress or strain wave, which propagates through an elastic medium. In general, the amount of energy released as an elastic wave depends on the initial conditions of the source. The rapid localized release of energy from the source generates elastic waves with frequencies in the ultrasonic range [22], which can be detected by an optical fiber or the PZT transducer sensor [23]. Elastic waves can be actively generated by actuators such as ultrasonic generators [24]. Normally, PZTs are designed and fabricated at a specific resonant frequency for ultrasound wave generator/sensor at frequencies less than 5 MHz.

For acoustic-ultrasonic detection, piezoelectric actuators are typically used for generating guided waves in the structure. Currently, piezoelectric transducers are state-of-the-art ultrasound sensors, that are routinely used to detect ultrasonic signals by converting pressure waves to measurable electrical signals. Piezoelectric crystals (quartz and ZnO), piezoceramics (barium titanate or BaTiO₃ and PZT), and piezoelectric polymers (polyvinylidene difluoride or PVDF) are popular choices of piezoelectric materials for highly sensitive ultrasound detection. Further, the output voltage can be displayed on a digital scope and transferred to computer from PZT probe [25]. Although piezoelectric ultrasound detectors were widely used in imaging, several technical constraints can potentially impede further development of medical imaging techniques as listed below.

2.1. Piezoelectric element size

In any kind of image sensing, high resolution measurements require the use of short wavelength acoustic signals, which requires detection and generation of high frequency ultrasound [26]. For instance, high resolution microscopes are based on the emission of UV-light, and the distinction between two points is limited by the optical wavelength via diffraction optics. Likewise, the imaging resolution of acoustic sensors is limited by the size of piezoelectric elements, which defines the acoustic wavelength that is often in millimeters to centimeters scale. The acoustic element size and installation position also affect the sensitivity of the sensor, as it is highly directional (wave polarization must be aligned with the sensor) and there is a spatial averaging effect for frequencies higher than MHz due to large sensor dimension. This can degrade the image signal to noise ratio for applications that require omnidirectional response such as photoacoustic imaging [27]. Omnidirectional microphones can pick up sound with equal gain/sensitivity from all sides or directions of the microphone, (i.e. whether a user speaks into the microphone from the front, back, left, or right side, the microphone will record the signals all with equal gain) [28]. However, unidirectional microphones can only pick up sound with high sensitivity from a specific side/direction.

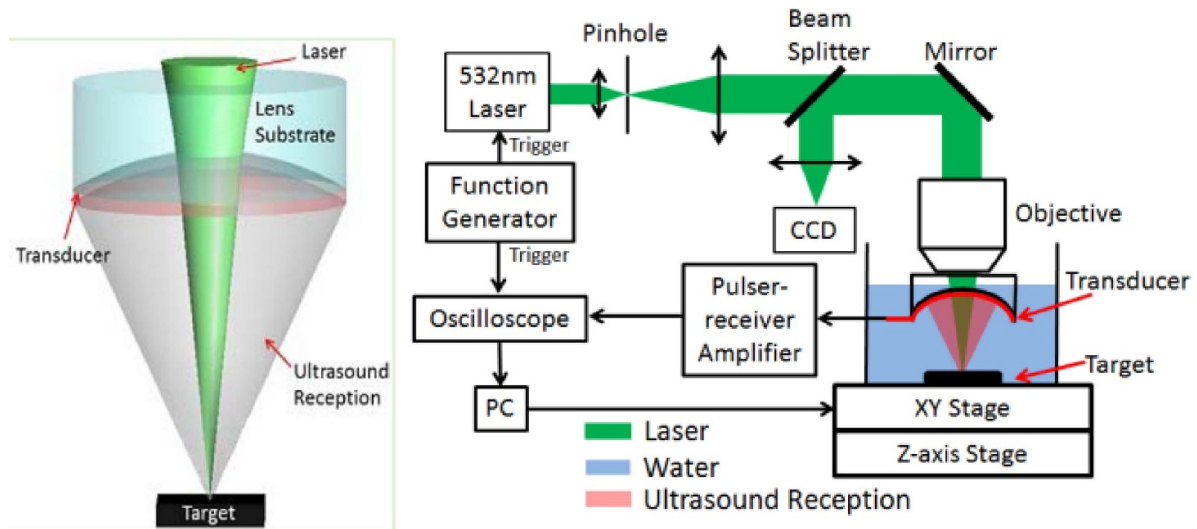


Figure 2. Photoacoustic microscopy setup with a focused transparent transducer (left), the setup for characterizing the optical and acoustic properties of focused transparent transducer (right). © [2020] IEEE. Reprinted, with permission, from [26].

2.2. Sensor material

The highest sensitivity with piezoelectric sensors requires detectors that are fabricated from acoustically resonant PZT materials. This can result in a sharply peaked frequency response thereby precluding a faithful representation of the incident acoustic wave and ultimately compromising image fidelity either for medical or NDT.

2.3. Detection bandwidth

The structural details in biological tissues have a scale of 1–200 μm , which requires a broad frequency range ultrasound detection from 7.5 MHz to 1.5 GHz in photoacoustic tomography (PAT) and photoacoustic microscopy (PAM). In recent years broadband response has been achieved by detecting combined optical and acoustic signals as transmitter and receiver [26], with PZT MEM [27] and PZT thin film [29].

(a) The approach proposed in [26] reports an integrative imaging setup consisting of both optical and acoustic components. Their synergistic operation is essential for obtaining optimal imaging performance. It is based on a focused optically transparent ultrasound transducer with a wide bandwidth for PAM, shown in figure 2. The transducer consists of a 9 μm -thick polyvinylidene fluoride (PVDF) film coated with Indium-tin oxide (ITO) and metal electrodes, which is laminated onto a concave glass lens. The transparent transducers can have adequate optical transmittance at the laser excitation wavelength for ultrasound signal generation and provide a complete sensing substrate for receiving the PA signal for a compact generation and detection scheme. The acoustic center frequency of 24 MHz, and an acoustic bandwidth of 26 MHz were demonstrated. With an acoustic numerical aperture (NA)

of 0.23, it provides a 0.13 mm acoustic focal spot and a 1.6 mm focal depth.

(b) The high frequency piezoelectric MEMS ultrasound transducers [27] were developed by the deposition of piezoelectric thin films on larger structures. This demonstrates good performance over very high frequencies, ranging from tens to hundreds of MHz, which is suitable for high-resolution imaging systems [29]. The dimensions of the transducers were 0.5 μm in thickness, 30 μm in width, and 150–300 μm in length. The chip consists of 16 channels of transmitter and receiver circuits, which include programmable pulse delay circuits, pre-amplifiers, variable gain amplifiers, 250 MHz analog-to-digital converter, and on-chip memory [30]. This broadband frequency response PZT device opens a door for high sensitivity optical imaging. Unfortunately, they require custom designed electronics and transducers, which makes it difficult to access for general use.

2.4. Limitation in optical resolution PAM

In medical imaging, the lateral resolution is determined by either ultrasound or optical focusing [5]. In acoustic-resolution imaging [31], the lateral resolution depends on the center frequency and NA of the ultrasound detector. In optical-resolution PAM, the lateral resolution is determined by the diffraction-limited optical focus, which is limited by the bulky and optically opaque piezoelectric detectors which forces imaging into transmission mode. Thus, this introduces another limitation: the sample thickness is an issue due to strong frequency-dependent acoustic attenuation [32].

In NDT and SHM monitoring, the fragile PZT materials associated thin film made them difficult to be used for high ultrasound frequency in field applications, which limits the spatial resolution of ultrasound imaging to the mm level. In

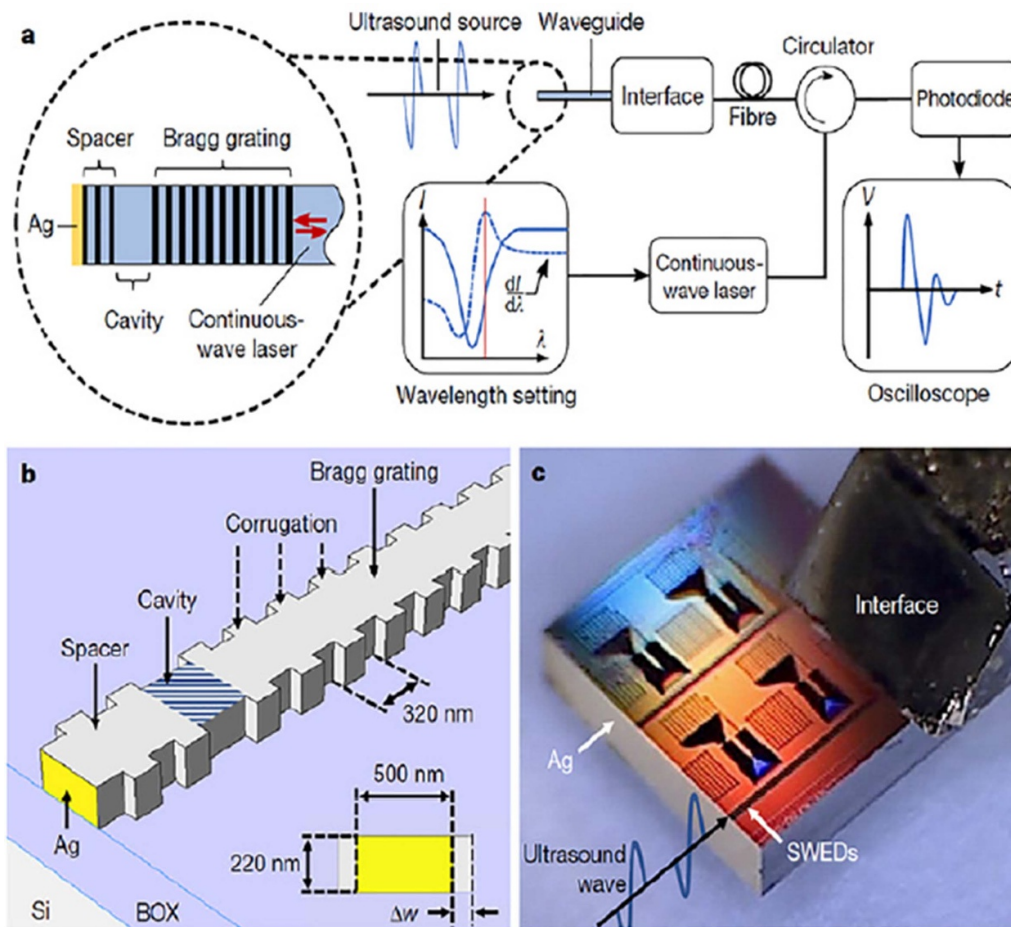


Figure 3. Silicon point-like silicon waveguide-etalon detector. Design and operating principles of the silicon waveguide-etalon detector (SWED). Reproduced from [27]. CC BY 4.0.

addition to the thickness of the PZT on maximum ultrasound frequency, the sensitivity of ultrasound sensors is reduced by the small contact area (the adhesive layer bonding) between the PZT sensors and the structure. To overcome the above limitation of PZT sensors in imaging and field monitoring, optical ultrasound sensors provide greater sensitivities over a significantly wider frequency range, hence potentially providing higher spatial resolution.

In 2020, Shnaiderman *et al* demonstrated a miniaturized high-sensitivity and ultra-broadband acoustic sensor based on an array of point like silicon waveguide-etalon detector using an SOI platform. The cavity is formed by a spacer and a Bragg grating. The size of the cavity size is 220 nm by 500 nm, which gives an ultra-small sensing area (figure 3). The SOI based optical cavity resonator provides per-area sensitivity to be 10^8 times better than that of piezoelectric detectors. This design enables an ultra-wide detection bandwidth, reaching 230 MHz at -6 dB [33]. The optical resonance enhanced the readout sensitivity of mechanical vibration, the mechanical resonance in optical micro-resonators also increases its response to an external ultrasound signal by increased interaction length of optical and mechanical wave enabled by multiple-interference due to low loss of optical wave, therefore increasing the sensitivity. The optical cavities depend on refractive index-induced

optical path length changes and static deformations rather than nano-mechanical resonances, while the peak shift sensitivity is enhanced by optical interference.

The small optical waveguide sensors, such as fiber or Si waveguide ultrasound sensors, offer a miniaturized, optically transparent, highly reliable and low-cost ultrasonic detector [34] based on optical phase changes from the ultrasound pressure induced refractive index changes in optical fibers. Such a change can be measured by optical interferometers, Fiber Bragg Gratings (FBGs) [35] and micro-fiber-based ultrasound sensors [36]. The combined optical and acoustic transducers allow higher sensitivity over broad frequency range, thus suitable for imaging of small dimensions through waveguides with micrometer and nanometer sizes. This allows a simpler and more compact imaging system configuration with optimal detection condition. The challenge of providing high strength ultrasound signals needed for better imaging quality requires the study of materials on impedance matching over broadband for ultrasound transmitter. The high optical and acoustic coupling in certain materials is stronger, the choice of the materials needs more research to search wide wavelength window optical transparent transducer. Since the photo-elastic effect has little frequency dependence, we can choose optically transparent materials for combined ultrasound generation and

detection. The heat dissipation can be an issue, as continuous high power optical pulse driving could lead to the fatigue of the transducer material. This will lower the photo-acoustic conversion ratio, which reduces the ultrasound power and lowers the image quality. Semiconductor coolers can help to mitigate this effect.

3. Fiber based interferometer for ultrasound sensing

Optical ultrasound sensors offer an alternative to piezoelectric sensors that have dominated the market for years, especially those based on fiber interferometers, such as Mach–Zehnder interferometers, F–P interferometers, microspheres, micro-rings, and in-fiber Bragg gratings as shall be detailed next. The fiber-based ultrasound sensors detect acoustic waves through the photo-elastic effect or acoustic pressure induced deformation on the refractive index, both change the optical path length in the interferometers. The changed optical path length can be detected by the time varied optical phase detection. Compared with optical waveguide ultrasound sensor, fiber-based sensors are easy to be packaged and compatible with telecom equipment. The massive production of fiber related telecom apparatuses made such sensors cheap and readily accessible.

Ultrasound wave induced displacement is very small, in the scale of nanometres [37], which is much smaller than the optical wavelength, say at 1550 nm, where the fiber loss is the smallest and optical components are the cheapest due to the common wavelength with the telecom industry. In optical interferometers, light is transmitted through the sensing path (SP) and reference path (RP) and is then recombined by an optical fiber coupler to produce interference signals. The optical path length difference between the RP and SP can be measured as a function of time, which is proportional to the acoustic wave induced displacement. In 1977 a double path Mach–Zehnder interferometer (MZI) was proposed to detect ultrasonic waves in water [38]. The sensing fiber was a coiled fiber submerged in an acoustic beam; the plane of the coil was parallel to the acoustic wavefronts. The single mode fiber elements used in this system were 4 m long to increase the sensitivity of acoustic detection of phase change. The coiled portion had a diameter of 3.3 cm. The two MZI beams were collimated and combined, generating an interference pattern carrying acoustic information that was detected by a photomultiplier at visible wavelength for a better signal to noise ratio.

Rashleigh [39] proposed a single fiber acoustic sensor based on the phase velocities of the polarization modes in a tension-coiled fiber due to acoustic wave induced differential changes, which resulted in the polarization rotation of the transmitted light, called a polarimetric optical fiber acoustic sensor. The acoustically induced birefringence in polarization maintaining fibers can be detected at high frequencies (>1 MHz) due to the anisotropic strain distribution [40]. At lower frequencies, the birefringence is attributed by the inhomogeneous elastic properties of the fiber. The first in-fiber Michelson interferometer (MI) for detecting vibration was demonstrated in 1980 [41]. Udd [42] presented the first

fiber-optic acoustic sensors based on Sagnac interferometers. Alcoz *et al* [43] demonstrated a short gauge length (5–13 mm) intrinsic Fabry–Perot interferometer, which can detect ultrasonic longitudinal waves of 0.1–5 MHz. The main difference between Michelson and Mach–Zehnder interferometers is that the interference is generated between the reflected light by the SP and RP in the former, and the transmitted light in the latter.

Glass optical fibers have a low opto-elastic coefficient. Therefore polymer materials, with large opto-elastic coefficients, can be used to improve the sensitivity of fiber sensors [44, 45]. For instance, graded-index (GI) polymer fiber sensor can provide over 20-fold improvement in sensitivity compared to its glass fiber counterpart [45]. Fabry–Perot interferometers (FPI) offer a significantly reduced gauge length as one thin slice of sensing material at the end of the fiber may act as a FPI with length equivalent to the period of an ultrasound frequency of 20 MHz [46], if it can be fabricated with soft materials of low Young's modulus.

The sensor gauge length is the major limitation of interferometric OFS for ultrasound, as medical diagnosis requires miniature device. At high frequency ultrasound waves (10–500 MHz level), the acoustic wavelength can be as small as a few μm depending on the acoustic frequency. To respond to small displacements associated with phase shifts induced by high frequency vibrations, the interferometers must have a short optical path and fast response, which are not available using optical fiber as ultrasound sensor.

Polymer materials are usually softer than dielectric materials, such as glass. They can be easily deformed by ultrasound waves, thus allowing for high sensitivity. Polymer-based F–P micro-resonators have been fabricated on the tip of the fiber via a solid plano-concave polymer microcavity formed between two highly reflective mirrors (figure 4) [47]. The cavity is embedded within an encapsulating layer of identical polymer to create an acoustically homogeneous planar structure. The cavity itself is constructed by depositing a droplet of optically clear UV-curable liquid polymer onto a dielectric mirror coated polymer substrate. The droplet stabilizes to form a smooth spherical cap under surface tension and is subsequently cured under UV light. The second dielectric mirror coating is then applied to create the encapsulating layer. Laser light is incident from the other end of the fiber to measure the acoustic wave induced deformation of the cavity. This plano-concave micro-resonator has achieved strong optical confinement with a Q factor of 105, and broad bandwidth up to 40 MHz.

Therefore, optical ultrasound sensors have several advantages over the piezoelectric counterpart, including: (a) *high sensitivity*. Optical fiber devices, such as FPI, FBGs, ring resonator and MZI can enhance the interaction length of optical and acoustic waves. The phase detection of the acoustically modulated optical waves can be detected at a high signal to noise ratio over a broader frequency range due to the high optical carrier frequency (10^{14} Hz), overcoming thermal noise or the shot noise limit. On the other hand, PZT devices operate in electronic noise limited regime, and carrier frequency is microwave frequency, which makes it highly frequency selective and have a narrow band; (b) *low directivity at MHz*

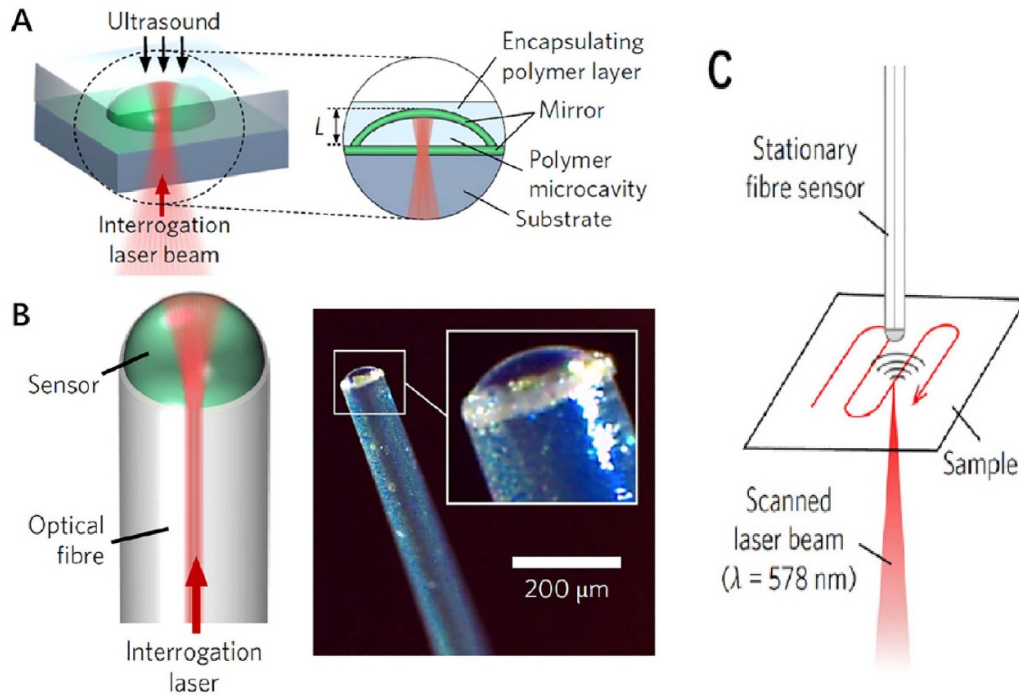


Figure 4. Acoustic sensor based on plano-concave F-P cavity. Reproduced from [47]. CC BY 4.0. (A) Diagram of the plano-concave polymer micro-resonator. (B) Micro-resonator fabricated at the end of the fiber for imaging applications. (C) Photoacoustic imaging by using the fiber connected plano-concave polymer micro-resonator.

frequencies. Optical fibers are microscale in size, so they can be packaged or integrated on a chip. They are easily fabricated with less requirements on acoustic impedance matching, offering low directivity detection of acoustic waves over wide bandwidths. (c) *Multiplexed sensing.* The widely developed multiplexing fiber sensor techniques can be adopted for fiber-based ultrasound sensors [7], as well as distributed ultrasound sensors [14]. Multiple fiber optic sensing probes will increase imaging speed and spatial coverage for NDT, SHM and medical applications with great potential for other applications in the ultrasound field.

4. FBG based ultrasound sensing

Interferometers from FBG with short gauge length are attractive for ultrasound sensing [48]. FBGs are spectrally reflective elements written into the core of optical fibers. The grating reflects a single wavelength of light, called the Bragg wavelength, defined as $\lambda_B = 2n_{\text{eff}}\Lambda$, Λ being the grating period and n_{eff} the effective refractive index of the fiber at the FBG. Under ultrasound modulation, both the acoustic wavelength and the effective index will be modulated, which leads to a shift of the Bragg wavelength. FBGs used for ultrasonic measurements were first demonstrated for medical applications [49], where the ultrasound signal was measured through the intensity change at quadrature point of the FBG spectrum. The upper acoustic frequency limit is set by the length of the grating, i.e. the grating length L_{FBG} should be less than half of the acoustic wavelength Λ_a in

the fiber core [50], i.e., $\frac{\Lambda_a}{L_{\text{FBG}}} > 2$. Suppose modulation of the refractive index $n_{\text{AC}} = 1.2 \times 10^{-4}$, $L_{\text{FBG}} = 2.12 \text{ mm}$, $\Lambda = 530.65 \text{ nm}$, $\lambda_B = 1534.97 \text{ nm}$ [51], this leads to $\Lambda_a > 4.2 \text{ mm}$. If we take the sound velocity in the fiber to be 5000 m/s , then the maximum acoustic frequency is approximately 1.25 MHz .

The jacket of an FBG fiber sensor also acts as a transducer, which can be made with special material to match the impedance of the measured structure or environmental medium (i.e. water) to enhance ultrasound response [52]. This transducer helps couple the ultrasound signal from the medium to the fiber ultrasound sensor. Takeda *et al* [53] developed a small diameter optical fiber with $40 \mu\text{m}$ cladding and $52 \mu\text{m}$ polyimide coating to improve the stress detection by the FBG from ultrasound wave. For the sensing of signals in the ultrasonic range, viscous coupling of the optical fiber to the structure provides an extremely high SNR, such as vacuum grease [54]. In the regime where $\Lambda_a/L_{\text{FBG}} \gg 1$, the FBG grating is subjected to uniform deformation, which leads to a shift of the Bragg wavelength proportional to the amplitude of the GW, which is the ultrasound pressure wave induced displacement. The recommended ratio for the reliable shift in the Bragg wavelength was determined to be between 6 and 7 [39]. Considering $\frac{\Lambda_a}{L_{\text{FBG}}} = 6$, the maximum detectable frequency drops to 417 kHz for 2 mm length of FBG sensor. This limits the size of the damage/cracking that can be detected with FBG sensors. The excitation frequency of Lamb waves is limited by the following condition: Λ_a must be smaller than the defect dimensions, which sets the FBG ultrasound response to $< 5 \text{ MHz}$ [51]. When we use FBGs to detect acoustic waves, the acoustic wavelength Λ_a should be comparable to the FBG length L_{FBG} ,

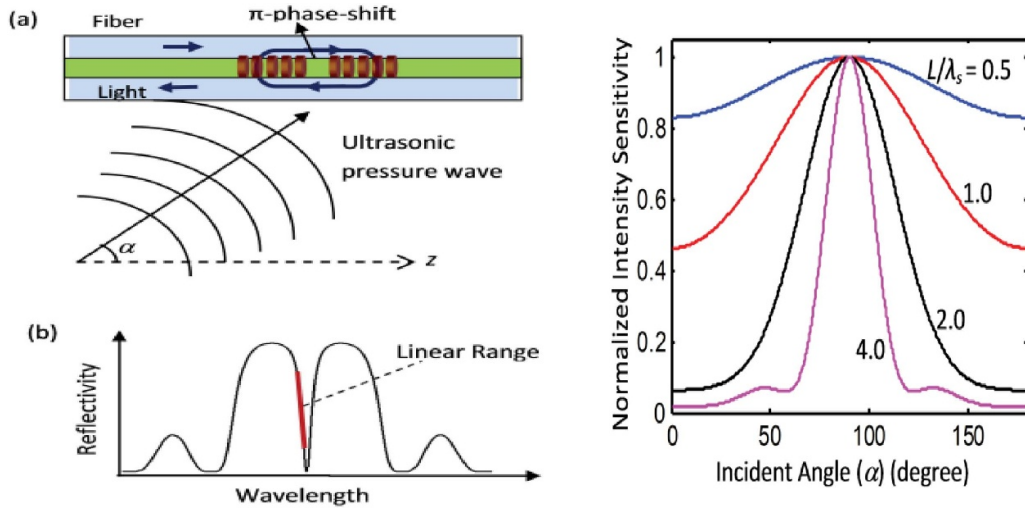


Figure 5. Pi-phase shift FBG ultrasound sensor. © [2012] IEEE. Reprinted, with permission, from [56]. On the left: (a) A π FBG under an ultrasonic pressure wave impinging onto the grating with an incident angle of α . (b) The reflection spectrum of a π FBG. On the right: Detected intensity (sensitivity) as a function of incident angle of ultrasound over $l = 4$ mm π FBG with a refractive index modification depth $\delta n = 2 \times 10^{-4}$ subjected to ultrasonic waves of different wavelength.

so that the stress induced by acoustic pressure is constant over L_{FBG} , which gives the shifted spectrum comparable to those without acoustic waves.

In MHz GW, Lamb wavelengths in thin metallic structures are in the order of millimeters, so that the detection of Lamb waves with typical FBGs with mm-length is given in the transition regime of $\frac{\lambda_a}{L_{\text{FBG}}} \approx 1$. In this case, the maximum detectable frequency is approximately 2.5 MHz. One can use an edge filter to detect intensity change [51] instead of the wavelength shift of FBG spectrum. In the edge filtering configuration the sensitivity of the FBG is proportional to the slope of the FBG reflectivity spectrum. Thus, modifying the index modulation of the FBG can improve the slope; ultrasound sensor operates at the maximum slope point for the highest intensity change detection by digital scope for direct intensity detection at the selected wavelength of FBG spectrum, through Fast Fourier Transform one can get frequency information. This process allows for real time ultrasound detection. FBGs's short length translates into a wide reflection bandwidth, which increases with decreased FBG length, limiting how accurately the spectral shift caused by acoustic waves can be determined. Considering typical $L_{\text{FBG}} = 2 - 10$ mm, the detection of acoustic waves is limited to frequencies in the range from a few hundred kHz to 1 MHz, corresponding to different reflection coefficients with different bandwidths of the FBGs. The widening of the peak is due to the non-uniform strain applied on the different parts of the FBG. When the edge filtering configuration is used, the detected intensity would correspond to the averaged value due to non-uniform strain applied along the FBG, preventing the measurement of higher acoustic frequencies. If multiple acoustic wavelengths fit within the FBG length, then we always detect the averaged intensity. The coupling mechanisms between the Bragg wavelength shift and the peak widening changes is measured at the different ratios at different GW frequency [55]. It is suggested that the FWHM peak width of the FBG spectrum may be used for MHz ultrasound

(GW) detecting, which would replace traditional FBG peak shift measurements.

FBG ultrasound sensors are mainly used for ultrasound non-destructive testing detection of cracks (sub-mm) in materials, as the FBG wavelength shift detection accuracy is limited by its bandwidth of a few GHz range. A phase-shifted fiber Bragg grating (PSFBG) is fabricated by inserting a π -phase in the middle of a traditional FBG, its spectrum property is shown in figure 5. For the pressure wave that impinges onto the π -FBG at an angle of α with respect to the fiber axis in figure 5(a), the measured ultrasonic wavelength along the fiber axis direction is increased with the following relation [56].

$$\lambda_a = \frac{\lambda_s (\text{wavelength of ultrasound})}{\cos \alpha}.$$

It was found that amplitudes of the refractive index and the grating pitch modifications induced by the ultrasonic pressure wave remained unchanged. It is likely that the directivity of a π FBG ultrasound sensor is highly dependent on the ratio between the grating length and the ultrasonic wavelength. This in fact imposes a limitation on the maximum detectable ultrasound frequency. The PSFBG network is formed by a π -FBG array at different wavelengths. The wavelength shifts of each PSFBG are detected by a tunable laser locked by integrating a proportional-integral-derivative controller [57]. This network can detect Lamb waves in composite laminate and evaluate cracks under loading. The optical demodulation of FBG sensors enabled a higher sensitivity than PZT ultrasound sensor. The ability of multiplexing FBG sensors offers multipoint detection, which makes them more attractive for NDT detection, whereas PSFBG can be at the same time much more expansive than PZT sensors. However, having numerous FBGs with a single demodulation unit makes the cost per sensor cheaper. In addition to their lightweight which is critical for NDT in aerospace, such as satellite and airplane,

even bridge monitoring will get benefit from numerous light-weight ultrasound sensors. We expect to see an increase in research and development, and the manufacturing of PSFBG acoustic sensors for industry applications in the coming years.

5. Micro- and nano-fiber and structured fiber device

Micro- and nanofiber photonics can greatly increase the upper frequency limit of ultrasound sensors. The extremely small size of the fiber couplers and fiber tapers means it is more feasible to embed the sensor in material systems with minimal disturbance to structural monitoring. This makes the microfiber ideal for in-service condition monitoring [7]. The coupling length of the structured micro- and nanofiber can range from a few μm to hundreds of μm , for instance, a small section ($L_{\text{microfiber}} = 100\text{--}120 \mu\text{m}$) of off-core fiber [36] was demonstrated to form a Fabry–Perot cavity-based ultrasound sensor with a frequency response from 5 kHz to 45 MHz. The ultrasound wave was generated by high order harmonics of PZT transducer with resonant frequency of $\approx 2\text{--}3$ MHz. The small amplitude displacement of high order harmonics in the generation process has set the upper frequency limit for fiber ultrasound sensors. To prove that the sensor is suitable for sensing higher acoustic frequencies, other methods of acoustic frequency generation must be explored. Due to the stronger attenuation of higher frequency ultrasound waves, these often correspond to smaller pressure changes, i.e. smaller displacements in the micro/nanofiber device. Hence, micro/nanofibers represent future trends for high-frequency acoustic wave detection, especially for impact wave location localization [58]. Compared with fiber end FPI cavity, the fiber taper, off-core fiber, and coupler type sensors have better bending capabilities, which is essential for deformation due to pressure waves from ultrasound [59]. Micro- and nanofibers have little loss in signal strength associated with a large range of tension and compression stress sensing [59], as the optical signal travels in optical fiber and air which bring the effective Young's modulus to be lower counting the combination of the optical path in glass and air through twist fiber taper [36], which has fast response time and recovery time from mechanical wave induced deformation. This can lead to high frequency ultrasound sensing. The bending capability is essential for the high frequency ultrasound sensor which is inversely proportional to the size of cracks.

Another factor contributing to ultrasound sensitivity is a low Young's modulus material for the sensor, as it is easy to be deformed for small displacement by optical wave. The SiO_2 fiber is made from glass that has a high Young's modulus. We need to design the sensor device with an effective low Young's modulus by making light propagate in two mediums: (a) normal silica fiber and (b) a medium that allows the fiber to bend easily. One approach is to make the 'optical fiber spring' between different off-core and on-core fiber sections, so that light travels between the air and optical fibers with lower effective Young's modulus. The deformations between

fiber sections enable multi-mode interference that changes the phase and amplitude of the light due to ultrasound induced pressure waves, which can be detected by measuring the time dependent intensity change.

For a 100 MHz ultrasound wave in glass, its acoustic wavelength is about $50 \mu\text{m}$. The displacement is likely in the order of $<1\%$ of the wavelength, in the range of nanometers (nm), which is much smaller than the optical wavelength. To further increase ultrasound frequency detection, we need to design fiber sensors with small dimensions in longitudinal length and transverse diameter, where ideally the size should be comparable to the ultrasound wavelength at the μm level. The free-space off-core fiber based FPI [36] has a $125 \mu\text{m}$ diameter, and a sensing length of $100 \mu\text{m}$. Fiber tapers (microfibers) can reduce the dimension of the cross section, and the length of the sensing fiber can be reduced by twisting two tapered fibers of different materials, such as an As_2Se_3 taper (refractive index $n = 2.9$) and a SiO_2 taper ($n = 1.46$) as shown in figure 6 [60]. This twisted fiber taper is $5 \mu\text{m}$ in diameter and is capable of sensing 94 MHz. The ultrasound generator is a PZT disc with resonant frequency of 3.7 MHz, where the 25th order harmonic was successfully detected.

The fused dual-core chalcogenide-PMMA microfibers is a good candidate for ultrasound sensors as the low Young's modulus in As_2Se_3 and PMMA (17.8 GPa for As_2Se_3 and 3.5 GPa for PMMA) [61] made deformation easier to detect when compared to silica. The strain sensitivity of the As_2Se_3 -PMMA taper is six times higher than that of silica-based tapers. This allows for highly sensitive broadband ultrasound sensing at 80 MHz.

The fiber optic ultrasound generator is based on the photoacoustic (PA) principle, which is an optical approach to generating ultrasound signals. The PA approach involves three steps: energy absorption, thermal expansion, and acoustic generation. The fiber optic ultrasonic generator converts pulsed laser energy exerted on the photoabsorptive thin films into thermoelastic waves. The center frequency and bandwidth of the generated ultrasound is determined by the incident laser pulse [62]. The fiber optic ultrasound generator can be fabricated with polydimethylsiloxane (PDMS) thin film in the end of a multi-mode fiber [63]. The size of each generation element is defined by the diameter of the fiber core. This fiber ultrasound transmitter can be used for corrosion monitoring [64], by the characterizing the samples at different corrosion rates. The ultrasound transmitter over 0.02–300 MHz frequency range is realized through polymer waveguides as shown in figure 7. The transducer is the curved adhesive waveguide on the off-core fiber of $100 \mu\text{m}$ enabled fiber-optic ultrasound transmitter at 306 MHz detection [65]. The ultrasound is generated by optical pulse excitation via photo absorption and thermal expansion of UV-cured adhesive, and then detected via the multi-mode interference of the same waveguide for the broad transverse acoustic waves. Because the same device can both generate and detect ultrasound resulting in more compact ultrasound probe, it offers new opportunities to the advanced biomedical, SHM and NDT.

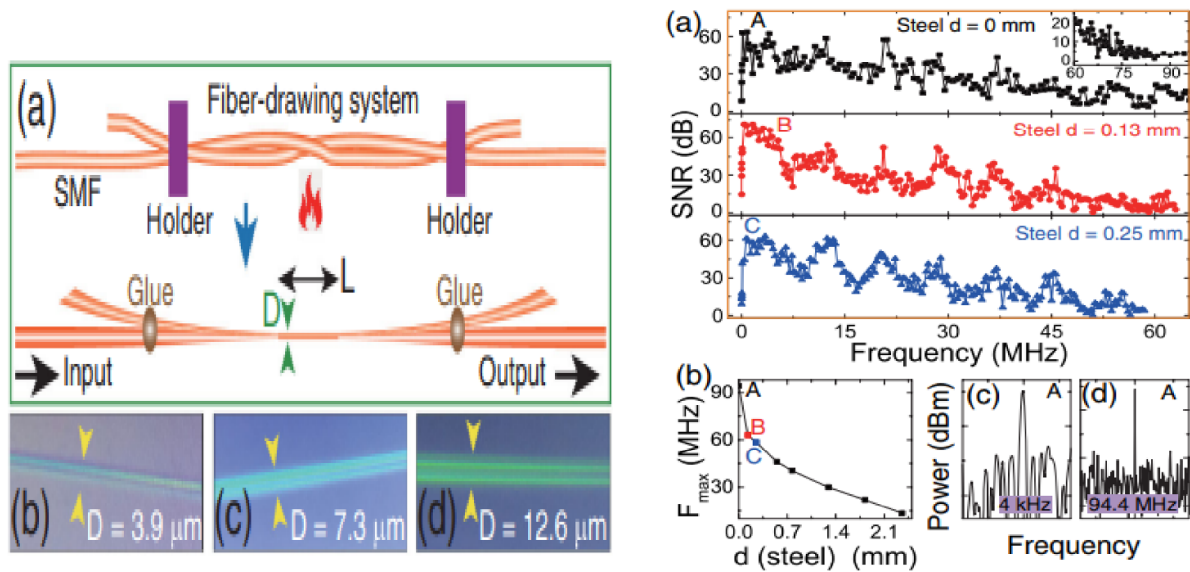


Figure 6. Micror-fiber ultrasound sensors. Reproduced with permission from [60]. [©The Optical Society]. Left: (a) fabrication of the twisted silica taper by fire drawing two twisted SMFs. (b)–(d) The three waist diameters. Right: (a) frequency responses with $D = 5 \mu\text{m}$ and $L = 5 \text{mm}$ under different steel thicknesses (d). Inset: frequency: 60 MHz to 95 MHz with sensor being attached to PZT. (b) Maximal detected ultrasound frequency (F_{max}) at different steel plate thickness. (c) and (d) At 4 kHz and 94.4 MHz with sensor attached to PZT.

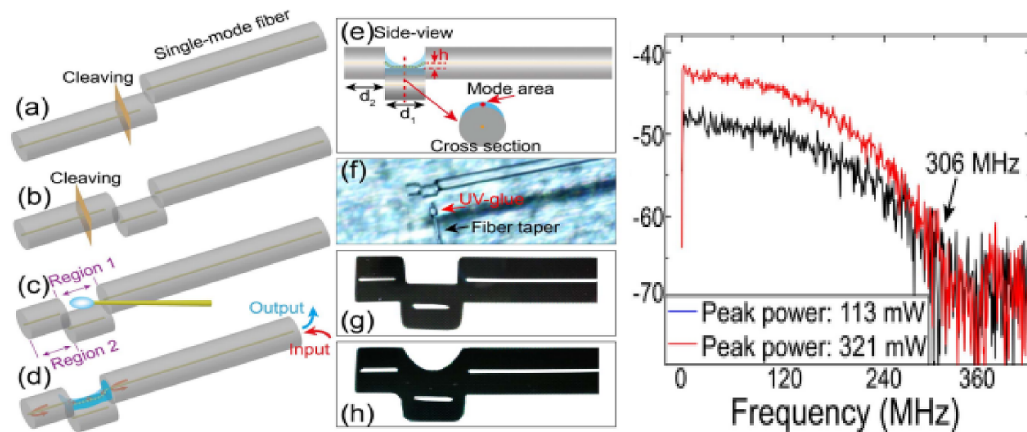


Figure 7. Ultrasound transmitter using the micro-fiber based on photo-acoustic generated ultrasound. © [2020] IEEE. Reprinted, with permission, from [65]. Left: (a)–(d) the fabrication of UV-cured adhesive waveguide between two fiber end-faces. (e) Cross-section of curved adhesive waveguide. (f) UV-cured adhesive dripping process. (g) and (h) side view before and after UV-cured adhesive. Right: ultrasound sensor power response in dB at different power of the pump laser.

The prospect of the micro- and nano-fiber device offers broadband ultrasound frequency response, which can be characterized by surface acoustic wave (SAW) generator over hundreds of MHz to GHz. High frequency SAWs can be generated through a pair of interdigital transducers (IDT) in a linear cavity configuration, where the cavity length defines its operating frequency [66]. The wave generated from the IDT device induces a strain oscillation that periodically changes the local length and refractive index of micro-fiber-based ultrasound sensors. This will provide a high frequency response for optical or fiber ultrasound sensor characterization. To overcome the narrow spectrum range of SAW resonance frequency, a sequence of IDT devices with different cavity lengths can be fabricated to cover broadband optical ultrasound sensors. This can be carried by optical/acoustic

Fabry–Perot spectrum, which was proposed in [67]. The package of SAW and micro-fiber will provide ultrasound transmitter and receiver, which is an alternative option of photo-acoustic ultrasound transmitters (figure 7).

6. Future prospects and conclusion

The ultrasound imaging systems are safe and portable, and offer high frame rates beyond 25 frames per second, which is the threshold for real-time display. Photoacoustic imaging is an emerging modality based on laser pulses delivered on tissues to produce ultrasound [5, 68, 69]. Photoacoustic imaging can penetrate the depth of tissues with high-resolution imaging of 100 μm limited by the bandwidth of PZT based

ultrasonic signal generation. This can be improved by laser-generated ultrasound (LGUS) [70] for high-frequency ultrasound with 100 MHz and a resolution of 20–30 μm [5].

LGUS in conjunction with optical detection of ultrasound allows for all-optical ultrasound systems. The all-optical platform offers unique advantages in providing high-resolution information and in facilitating the construction of miniature probes using fiber-based ultrasound sensors as mentioned in previous sections. The fiber optical detection platform intrinsically facilitates broadband ultrasound detection up to hundreds of MHz. Because the acoustic excitation mechanism is based on photoacoustic effect from thermoelastic approach of laser excitation, it is very different from the resonant characteristics of piezoelectric transducers. Therefore, they are promising for high-resolution ultrasound imaging due to flat spectral response in fiber optic ultrasound sensors.

The detection sensitivity of fiber ultrasound sensors is independent of their active area so long as the sensor dimension is comparable to the acoustic wavelength. High sensitivity is thus preserved with a small active area.

The application of SHM requires an extremely large number of point sensors. Benefiting from the technology offered by the telecom industry with various multiplexing techniques, fiber sensor networks with significant number of sensors can be developed with a single interrogation system and minimum modification for SHM and medical imaging. The overall cost of the sensing system can be cheaper compared with current PZT based ultrasound solutions. The potential of using the same device for generation and detection makes the fiber system [49, 50] especially attractive for SHM, NDT and medical imaging.

The future directions for applications of ultrasound sensor in imaging, NDT and SHM can be:

- (a) Nanocomposites with high photoacoustic conversion can be good materials for high-amplitude (strength) laser ultrasound generation. Further research in optimization and safety for medical usage of these nanocomposites are needed in advanced diagnostic and therapeutic applications.
- (b) The future research of fiber-optic ultrasound transmitters for interventional imaging and therapy should focus on their biocompatibility and safety. Particularly, reducing side effects and ensuring a safe delivery of strong laser pulses are key issues.
- (c) Development of a high-speed imaging system for medical and SHM is a valuable research direction for the future. Multiplexing fiber ultrasound networks will provide an efficient way to realize high-speed imaging over a large imaging sample.
- (d) The most current research in this field is still in basic research stage with proof-of-concept demonstration. More clinical and field tests should be conducted for real applications.
- (e) The advancements of research with micro- and nanofibers have the potential to reduce the cross section and length of conventional telecom fibers, allowing ultrasound sensors

with smaller dimensions and much higher ultrasound frequency detection for even higher imaging resolution.

Data availability statement

No new data were created or analysed in this study.

Acknowledgments

The author would like to acknowledge the useful discussion and suggestion from Dr Pedro Tovar, Gerard Tatel, Dr Liang Chen, and Elyse D'Aoust on this paper.

Funding

Natural Sciences and Engineering Research Council of Canada (DG-2020-06302, STPGP 506628); Canada Research Chairs (75-67138).

ORCID iD

Xiaoyi Bao  <https://orcid.org/0000-0002-5525-0694>

References

- [1] Twyman F and Dowell J H 1923 The optical sonometer *J. Sci. Instrum.* **1** 12
- [2] Dalecki D and Hocking D C 2016 Advancing ultrasound technologies for tissue engineering *Handbook of Ultrasonics and Sonochemistry* (Singapore: Springer) pp 1101–26
- [3] Chen S L 2017 Review of laser-generated ultrasound transmitters and their applications to all-optical ultrasound transducers and imaging *Appl. Sci.* **7** 25
- [4] Meixner M, Foerst P and Windt C W 2021 Reduced spatial resolution MRI suffices to image and quantify drought induced embolism formation in trees *Plant Methods* **17** 38
- [5] Wang L V and Hu S 2012 Photoacoustic tomography: *in vivo* imaging from organelles to organs *Science* **335** 1458–62
- [6] Shung K K, Cannata J M and Zhou Q F 2007 Piezoelectric materials for high frequency medical imaging applications: a review *J. Electroceramics* **19** 141–7
- [7] Soman R, Wee J and Peters K 2021 Optical fiber sensors for ultrasonic structural health monitoring: a review *Sensors* **21** 7345
- [8] Le J L, Robert S, Lopez Villaverde E and Prada C 2016 Plane wave imaging for ultrasonic non-destructive testing: generalization to multimodal imaging *Ultrasonics* **64** 128
- [9] Mitra M and Gopalakrishnan S 2016 Guided wave based structural health monitoring: a review *Smart Mater. Struct.* **25** 053001
- [10] Forgarty E 2023 *What is an Acoustic Wave? All the Science* (available at: www.allthescience.org/what-is-an-acoustic-wave.htm)
- [11] Murukeshan V M and Ta L H 2014 Hybrid-modality high-resolution imaging: for diagnostic biomedical imaging and sensing for disease diagnosis *Proc. SPIE* **9268** 92680U
- [12] Kao C K and Hockham G A 1986 Dielectric fiber surface waveguides for optical frequencies *Proc. IEEE* **113** 1151–8
- [13] Udd E (ed) 1991 *Fiber Optic Sensor* (New York: Wiley)

- [14] Bao X, Zhou D P, Baker C and Chen L 2017 Recent development in the distributed fiber optic acoustic and ultrasonic detection *J. Lightwave Technol.* **35** 3256–67
- [15] Zhu T, He Q, Xiao X and Bao X 2013 Modulated pulses based distributed vibration sensing with high frequency response and spatial resolution *Opt. Express* **21** 2953–63
- [16] Qin Z, Chen L and Bao X 2014 Distributed vibration/acoustic sensing with high frequency response and spatial resolution based on time-division multiplexing *Opt. Commun.* **331** 287–90
- [17] Lee J R and Tsuda H 2006 Sensor application of fibre ultrasonic waveguide *Meas. Sci. Technol.* **17** 645–52
- [18] Lee J R and Tsuda H 2005 Fiber optic liquid leak detection technique with an ultrasonic actuator and a fiber Bragg grating *Opt. Lett.* **30** 32935
- [19] Fomitchov P, Murray T W and Krishnaswamy S 2002 Intrinsic fiber-optic ultrasonic sensor array using multiplexed two-wave mixing interferometry *Appl. Opt.* **41** 1262–6
- [20] Gabai H, Steinberg I and Eyal A 2015 Multiplexing of fiber-optic ultrasound sensors via swept frequency interferometry *Opt. Express* **23** 18915–24
- [21] Atique S, Betz D, Culshaw B, Dong F, Park H S, Thursby G and Sorazu B 2004 Detecting ultrasound using optical fibres *J. Opt.* **33** 231–8
- [22] Scruby C B 1987 An introduction to acoustic emission *J. Phys. E: Sci. Instrum.* **20** 946–53
- [23] Tressler J F, Alkoy S and Newnham R E 1998 Piezoelectric sensors and sensor materials *J. Electroceramics* **2** 257–72
- [24] Jeon Y B, Sood R, Jeong J H and Kim S G 2005 MEMS power generator with transverse mode thin film PZT *Sens. Actuators A* **122** 16–22
- [25] Eaton M, Pullin R, Holford K, Evans S, Featherston C and Rose A 2009 Use of macro fibre composite transducers as acoustic emission sensors *Remote Sens.* **1** 68–79
- [26] Fang C, Hu H and Zou J 2020 A focused optically transparent PVDF transducer for photoacoustic microscopy *IEEE Sens. J.* **20** 2313–9
- [27] Li B B, Ou L, Lei Y and Liu Y C 2021 Cavity optomechanical sensing *Nanophotonics* **10** 2799–832
- [28] Learning about electronics 2018 (available at: www.learningaboutelectronics.com/Articles/What-are-omnidirectional-microphones)
- [29] Zhou Q F, Lau S, Wu D and Shung K K 2011 Piezoelectric films for high frequency ultrasonic transducers in biomedical applications *Prog. Mater. Sci.* **56** 139–74
- [30] Mina I G, Kim H, Kim I, Park S, Choi K, Jackson T, Tutwiler R and Trolrier-mckinstrey S 2007 High frequency piezoelectric MEMS ultrasound transducers *IEEE Trans. Ultrason. Ferroelectr. Freq. Control* **54** 2422–30
- [31] Zhang H F, Maslov K, Stoica G and Wang L V 2006 Functional photoacoustic microscopy for high resolution and noninvasive *in vivo* imaging *Nat. Biotechnol.* **24** 848–51
- [32] Strohm E M, Berndt E S L and Kolios M C 2013 High frequency label-free photoacoustic microscopy of single cells *Photoacoustics* **1** 49–53
- [33] Shnaiderman R, Wissmeyer G, Ulgen O, Mustafa Q, Chmyrov A and Ntziachristos V 2020 A submicrometre silicon-on-insulator resonator for ultrasound detection *Nature* **585** 372–8
- [34] Morris P, Hurrell A, Shaw A, Zhang E and Beard P 2008 A Fabry-Perot fiber-optic ultrasonic hydrophone for the simultaneous measurement of temperature and acoustic pressure *J. Acoust. Soc. Am.* **125** 3611–22
- [35] Wild G and Hinckley S 2008 Acousto-ultrasonic optical fiber sensors: overview and state-of-the-art *IEEE Sens. J.* **8** 1184–93
- [36] Fan H, Zhang L, Gao S, Chen L and Bao X 2019 Ultrasound sensing based on an in-fiber dual-cavity Fabry–Perot interferometer *Opt. Lett.* **44** 3606–9
- [37] Bucaro J A, Dardy H D and Carome E F 1977 Optical fiber acoustic sensor *Appl. Opt.* **16** 1761–2
- [38] Chao C Y, Ashkenazi S, Huang S W, O'Donnell M and Guo L J 2007 High-frequency ultrasound sensors using polymer microring resonators *IEEE Trans. Ultrason. Ferroelectr. Freq. Control* **54** 957–65
- [39] Rashleigh S C 1980 Acoustic sensing with a single coiled monomode fiber *Opt. Lett.* **5** 392–4
- [40] Chiang K S, Chan H L W and Gardner J L 1990 Detection of high frequency ultrasound with a polarization-maintaining fiber *J. Lightwave Technol.* **8** 1221–7
- [41] Imai M, Ohashi T and Ohtsuka Y 1980 Fiber-optic Michelson interferometer using an optical power divider *Opt. Lett.* **5** 418–20
- [42] Udd E 1983 Fiber-optic acoustic sensor based on the Sagnac interferometer *Proc. SPIE* **425** 90
- [43] Alcoz J J, Lee C E and Taylor H F 1990 Embedded fiber-optic Fabry-Perot ultrasound sensor *IEEE Trans. Ultrason. Ferroelectr.* **17** 302–6
- [44] Grun H, Berer T, Puhlinger K, Nuster R, Paltauf G and Brugholzer P 2010 Polymer fiber detectors for photoacoustic imaging *Proc. SPIE* **7564** 75640M
- [45] Gallego D and Lamela H 2011 High sensitivity interferometric polymer optical fiber ultrasound sensors for optoacoustic imaging and biomedical application *Proc. SPIE* **7753** 775370
- [46] Nuster R, Gratt S, Passler K, Grun H, Berer T, Burgholzer P and Paltauf G 2009 Comparison of optical and piezoelectric integrating line detectors *Proc. SPIE* **7177** 71770T
- [47] Guggenheim J A *et al* 2017 Ultrasensitive plano-concave optical microresonators for ultrasound sensing *Nat. Photon.* **11** 714–9
- [48] Kashyap R 1999 *Fiber Bragg Gratings* (New York: Academic)
- [49] Fisher N E, Surowiec J, Webb D J, Jackson D A, Gavrilov L R, Hand J W, Zhang L and Bennion I 1997 In-fiber Bragg gratings for ultrasonic medical applications *Meas. Sci. Technol.* **8** 1050–4
- [50] Webb D J, Surowiec J, Sweeney M, Jackson D A, Gavrilov L R, Hand J W, Zhang L and Bennion I 1996 Miniature fiber optic ultrasonic probe *Proc. SPIE* **2839** 76–80
- [51] Betz D C, Thursby G, Culshaw B and Staszewski W J 2006 Identification of structural damage using multifunctional Bragg grating sensors: i. Theory and implementation *Smart Mater. Struct.* **15** 1305
- [52] Moccia M, Consales M, Iadicicco A, Pisco M, Cutolo A, Galdi V and Cusano A 2012 Resonant hydrophones based on coated fiber Bragg gratings *J. Lightwave Technol.* **30** 2472–81
- [53] Takeda N, Okabe Y, Kuwahara J, Kojima S and Ogisu T 2005 Development of smart composite structures with small-diameter fiber Bragg grating sensors for damage detection: quantitative evaluation of delamination length in CFRP laminates using Lamb wave sensing *Compos. Sci. Technol.* **65** 2575–87
- [54] Cranch G, Johnson L, Algren M, Heerschap S, Miller G A, Marunda T S and Holtz R L 2017 Crack detection in riveted lap joints using fiber laser acoustic emission sensors *Opt. Express* **25** 19457–67
- [55] Goossens S, Berghmans F and Geernaert T 2020 Spectral verification of the mechanisms behind FBG-based ultrasonic guided wave detection *Sensors* **20** 6571
- [56] Liu T and Han M 2012 Analysis of pi -phase-shifted fiber Bragg gratings for ultrasonic detection *IEEE Sens. J.* **12** 2368–73

- [57] Wang R, Wu Q, Xiong K, Ji K, Zhang H and Zhai H 2019 Phase-shifted fiber bragg grating sensing network and its ultrasonic sensing application *IEEE Sens. J.* **19** 9790–7
- [58] Fu T, Liu Y, Lau K T and Leng J 2014 Impact source identification in a carbon fiber reinforced polymer plate by using embedded fiber optic acoustic emission sensors *CompositesB* **66** 420–9
- [59] Fan H, Chen L and Bao X 2020 Combined compression-tension strain sensor over $1 \mu\epsilon$ – $20 m\epsilon$ by using non-uniform multiple-core-offset fiber *Opt. Lett.* **45** 3143–6
- [60] Fan H, Ma W, Chen L and Bao X 2020 Ultracompact twisted silica taper for 20 kHz to 94 MHz ultrasound sensing *Opt. Lett.* **45** 3889–92
- [61] Wang H, Baker C, Kelly L, Tovar P, Chen L and Bao X 2022 Broadband ultrasound sensing based on fused dual-core chalcogenide-PMMA microfibers *Opt. Express* **30** 8847–56
- [62] Wu N, Wang W, Tian Y, Guthy C and Wang X 2010 Theoretical analysis of a novel ultrasound generator on an optical fiber tip *Proc. SPIE* **7677** 252–8
- [63] Zou X, Wu N, Tian Y and Wang X 2013 Non-destructive characterization for PDMS thin films using a miniature fiber optic photoacoustic probe *Proc. SPIE* **8694** 86940P
- [64] Zou X, Schmitt T, Perloff D, Wu N, Yu T Y and Wang X 2015 Non-destructive corrosion detection using fiber optic photoacoustic ultrasound generator *Measurement* **62** 74–80
- [65] Fan H, Chen L and Bao X 2020 Fiber-optic ultrasound transmitter based on multi-mode interference in curved adhesive waveguide *IEEE Photonics Technol. Lett.* **32** 325–8
- [66] Kelly L, Northfield H, Rashid S, Bao X and Berini P 2022 Fabrication of high frequency SAW devices using tri-layer lift-off photolithography *Microelectron. Eng.* **253** 111671
- [67] Kelly L, Berini P and Bao X 2022 Measuring velocity, attenuation, and reflection in surface acoustic wave cavities through acoustic fabry–pérot spectra *IEEE Trans. Ultrason. Ferroelectr. Freq. Control* **69** 1542–8
- [68] Davies S J, Edwards C, Taylor G S and Palmer S B 1993 Laser-generated ultrasound: its properties, mechanisms and multifarious applications *J. Phys. D: Appl. Phys.* **26** 329
- [69] Majlesi J and Unalan H 2004 High-power pain threshold ultrasound technique in the treatment of active myofascial trigger points: a randomized, double-blind, case-control study *Arch. Phys. Med. Rehabil.* **85** 833–6
- [70] Westerveld W J, Mahmud-Ul-Hasan M, Shnaiderman R, Ntziachristos V, Rottenberg X, Severi S and Rochus V 2021 Sensitive, small, broadband and scalable optomechanical ultrasound sensor in silicon photonics *Nat. Photon.* **15** 341–5